System Characterization and Analysis of the Multispectral Aerial Passive Polarimeter System (MAPPS).

Brent D. Bartlett and Jason F. Faulring and Carl Salvaggio

Rochester Institute of Technology, Chester F. Carlson Center for Imaging Science, Digital Imaging and Remote Sensing Laboratory, Rochester, NY, USA

ABSTRACT

Passive polarimetery has been used for many different remote sensing applications and can provide useful signatures for certain types of phenomenology. While broadband polarimeters have many advantages, such as high signal-to-noise ratio and small ground sample distance, there has been growing interest in the development of algorithms that take advantage of both spectral and polarimetric signals. The Multispectral Aerial Passive Polarimeter System (MAPPS) aims to produce multispectral polarimetric imagery of test scenes that can be used in algorithm development efforts and phenomenology studies. Preliminary data is presented along with a calibration and processing workflow that produces registered spectral Stokes imagery.

Keywords: multispectral,polarimetry,polarization,stokes,imagery

1. INTRODUCTION

For many years, the remote sensing community has been able to develop and test many algorithms on synthetic imagery created through the use of such tools as the Digital Imaging and Remote Sensing Image Generation model.[1] This approach allows for relatively easy exploration of many variables such as scene content, collection geometry, and platform parameters. While using simulated data has it's advantages, all operational algorithms must be able to perform well with data collected by real sensors. Many sensors over the years have provided the academic research community with test data of different modalities such as LANDSAT,[2] AVIRIS,[3] and POLDER[4] which provide multispectral, hyperspectral, and polarimetric data, respectively. While there are test scenes available that provide a comprehensive set of ground truth data for testing and evaluation purposes in general for multi- and hyperspectral data,[5] there is a lack of high resolution airborne test data available using the spectro-polarimetric modality. As new approaches for exploiting spectro-polarimetric data are developed, it is the aim of the Multispectral Aerial Passive Polarimeter System (MAPPS) to collect data that can be used to test new algorithms, validate modeling efforts, and explore new phenomenology.

2. SYSTEM OVERVIEW

The system requirements that were defined for this sensor include enabling research that explores the use of different spectral bandpass and polarimetric filters to create high resolution spectro-polarimetric imagery while maintaing low system design and operating costs. To meet these requirements, a division of time design was used to fabricate MAPPS out of OEM parts that can be commercially obtained and assembled with as little custom integration as possible. This keeps the system cost low and will allow for the largest amount of data to be collected at the lowest expense. It was determined that a high resolution JAI BM-500GE CCD camera with a Schneider Optics lens coupled to a Sutter Lambda 10-3 dual filter wheel with ten slots per wheel met the system requirements. The digital camera acquires 12-bit imagery with a resolution of 2456x2058 pixels with a 3.45um pixel pitch using a 35mm focal length giving high spatial resolution. The system optics are comprised of a color corrected achromatic lens which maintains a constant depth of field over the visible / near infrared spectral range so that the lens does not require refocusing as different bandpass filters are used. The first filter wheel contains a set of linear polarizers, each oriented with their transmission axes rotated relative to each other. The rotational alignment of these filters will be discussed in Section 2.1. The second filter wheel contains a set of spectral bandpass filters allowing for up to 10 different spectral bands to be collected. For each spectral filter the linear polarizer set is rotated, thus allowing for spectral Stokes imagery to be generated. Each image acquisition is triggered via a hardware TTL pulse

Further author information: E-mail: salvaggio@cis.rit.edu, Telephone: 1 585 475 6380

Polarization Science and Remote Sensing V, edited by Joseph A. Shaw, J. Scott Tyo,
Proc. of SPIE Vol. 8160, 81600A · © 2011 SPIE · CCC code: 0277-786X/11/$18 · doi: 10.1117/12.892327

from the filter wheel and written to one of three solid state hard drives via multi-threaded control software that has been developed in C++. Currently the system is able to acquire an image every 180ms which minimizes spatial shifting and atmospheric variance between frames to allow for accurate image registration during post-processing. The camera and filter wheel are held using a custom housing that keeps the camera focal plane aligned to the filter wheel and which allows for mounting onto either a tripod or a standard aerial shock mount. The housing can also be used to secure an inertial measurement unit to MAPPS allowing for system orientation to be determined. This information will be critical for the tasks of georeferencing any collected airborne imagery as well as providing collection geometries for processing of the polarimetric data. Figure 1 shows a top view of the system as well as the system mounted to a tripod.

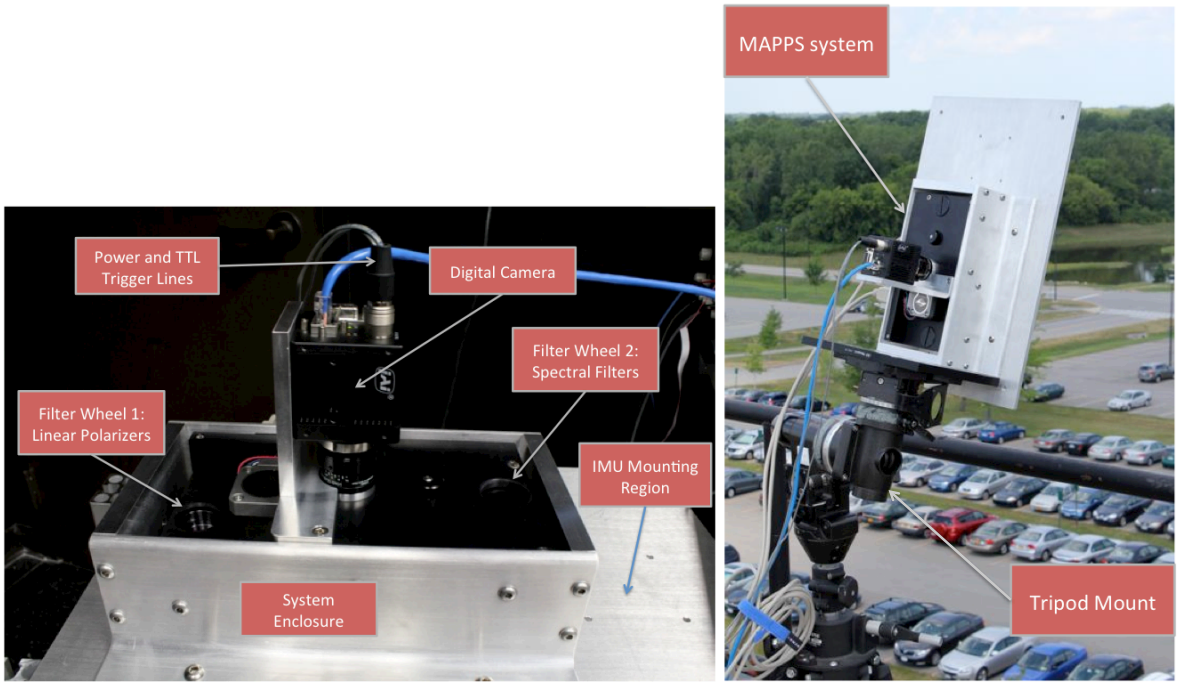

(a) MAPPS system (b) MAPPS system mounted on a tripod

Figure 1: MAPPS system consisting of a dual filter wheel and gigabit ethernet camera

Up to ten different types of spectral and polarimetric filters can be chosen for the system. The spectral filter set chosen for this preliminary system were chosen to closely match the spectral response of six of the spectral bands of the current generation WorldView 2 satellite.[6] Six filters were chosen from the standard filter catalog of Semrock allowing for interesting comparative studies to be performed between the space-based WorldView 2 sensor and the MAPPS system. The polarization filter set consists of four linear polarizers which were chosen to allow for four different polarizer orientations. The VersaLight series of polarization filters available from Meadowlark were chosen which provide good spectral transmission and contrast ratio across the spectral range required by the spectral bandpass filters. Figure 2 shows a plot of each spectral filter along with the nominal transmission of the linear polarizers.

2.1 Polarizer Alignment

One of the most challenging aspects in creating this type of spectro-polarimetric instrument is aligning each linear polarizer to the desired angular orientation. It has been shown that using four linear polarizers can simplify the measurement process[7] and as such the standard angle set of $\theta = [0°, 45°, 90°, 135°]$ was chosen. An alignment assembly was created that holds the MAPPS system in line with an OL-455 integrating sphere, a motorized rotation stage, and a reference linear polarizer. The motorized rotation stage is controlled via a micro-stepping motor controller which when combined with the rotation stage's gear ratio has a step size of $0.002 \frac{mrad}{microstep}$ allowing for very accurate positioning of the reference polarizer. Figure 3 shows this assembly with the MAPPS sensor placed on top.

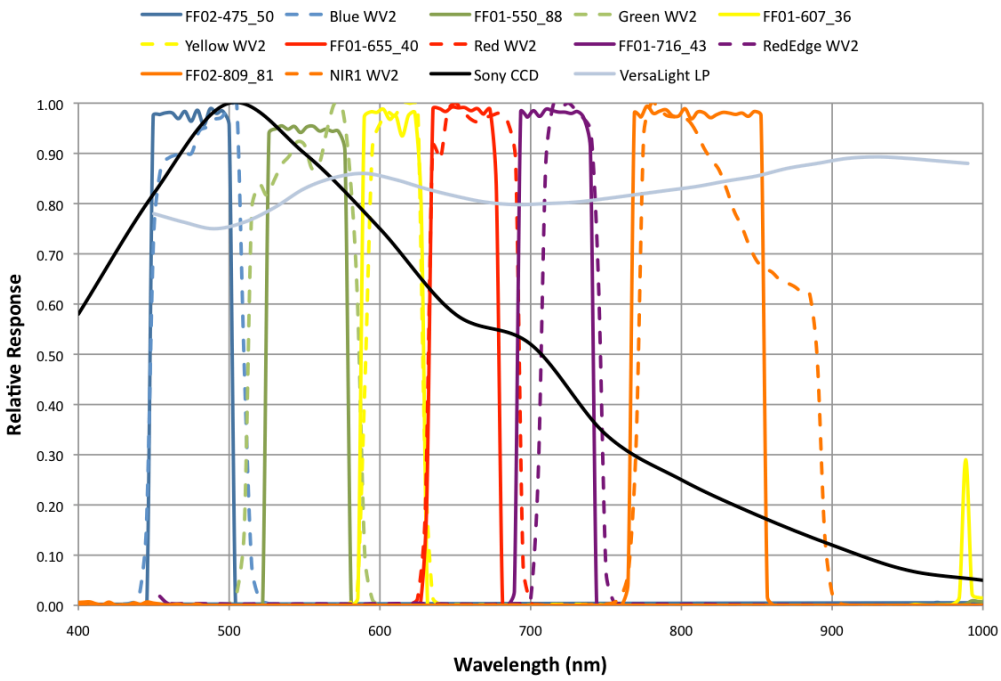

Figure 2: Relative spectral responses of Semrock bandpass filters and Meadowlark linear polarizers used in the MAPPS system. Corresponding WorldView 2 spectral bands are shown for reference.

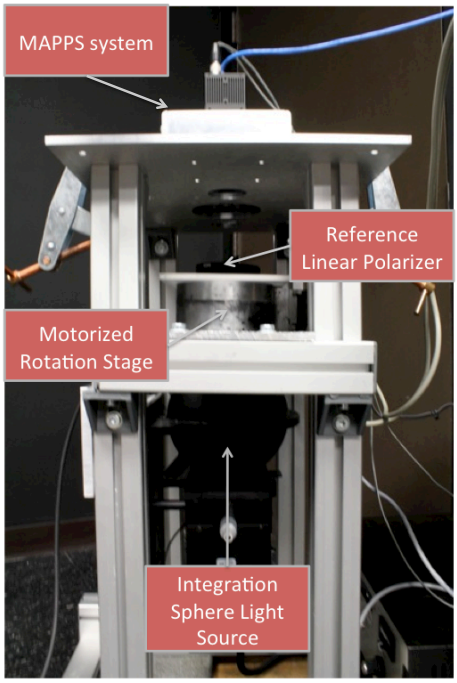

Figure 3: Calibration assembly used for filter alignment and system calibration.

Each linear polarizer in the MAPPS system was then aligned by first tightening each filter cup into the desired wheel slot. The reference polarizer was positioned to the desired angle with the motorized stage and the filter was then aligned by rotating it until the observed intensity was at a maximum. The filter in the MAPPS system was rotated by using a custom vacuum alignment tool which allowed for easy rotation of the filter by hand while in the filter wheel. After the filter was aligned, it was secured into place using a silicone adhesive and a retaining ring. The alignment was then checked by driving the reference linear polarizer via the rotation stage through a set of angles ranging from $[0^\circ - 180^\circ]$. If the filter was aligned it should exhibit a cosine response, peaked at the desired angle. This process was repeated for each of the two remaining filters. To check that no shifting occurred during the process of tightening the filter retaining ring, an alignment check was performed again for each filter. If the filter was aligned properly, then the intensity should peak at the desired angle for that filter. Figure 4 shows the results of the alignment check where each filter is within one degree of the desired angular orientation.

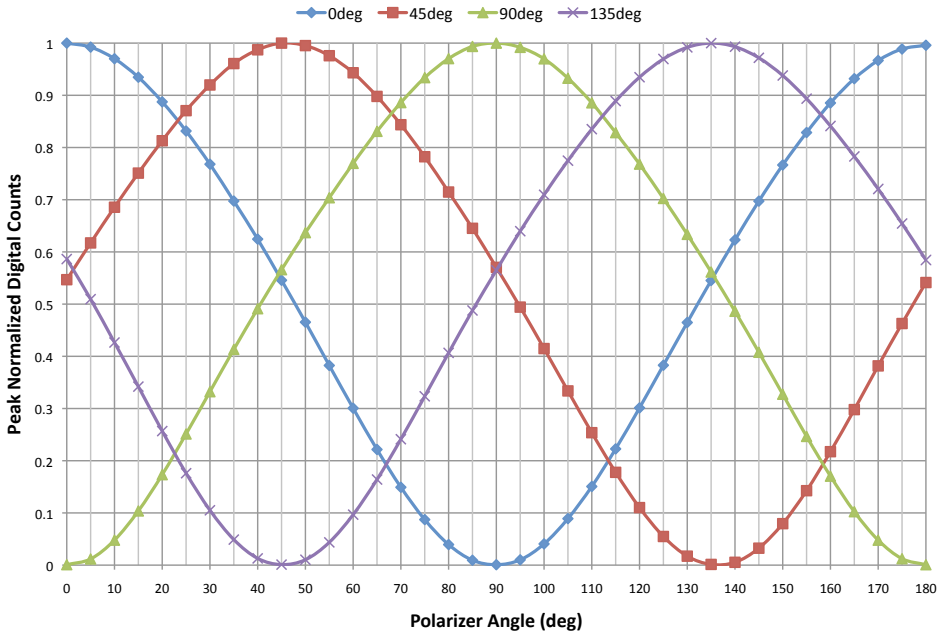

Figure 4: Filter alignment results performed by rotation of the reference linear polarizer.

2.2 Polarimetric Calibration

After alignment of the linear polarizers in the filter wheel housing a polarimetric calibration was performed. This calibration empirically measures the system Mueller matrix which will account for any residual misalignment of the polarizers, polarizer leakage, and additional polarization effects due to the spectral bandpass filters and optics. To accomplish this, imagery of the reference polarizer was collected as it moved to several different angular orientations. The system response for a given polarizer angle and spectral band can then be expressed through the following governing equation,[8]

$$\mathbf{X}_\lambda = \mathbf{A}_\lambda \cdot \mathbf{S}_\lambda$$

where $\mathbf{X}_\lambda$ is the (4×1) vector observed by the system, $\mathbf{A}_\lambda$ is the system matrix, and $S_{i\lambda}$ is the (3×1) input Stokes vector. If measurements at Q different reference polarizer angles are made the equation can be generalized into the following,

$$\mathbf{Y}_\lambda = \mathbf{A}_\lambda \cdot \mathbf{T}_\lambda$$

where $\mathbf{Y}_\lambda$ is now a $(4 \times Q)$ matrix containing measurements of the reference polarizer for each of the Q angular orientations and $\mathbf{T}$ is a $(3 \times Q)$ matrix containing the corresponding known input signals. An estimate of the $\mathbf{A}_\lambda$ can now be found by using the pseudo inverse of $\mathbf{T}_\lambda$,

$$\mathbf{T}_\lambda^{\#} = \left(\mathbf{T}_\lambda^T \cdot \mathbf{T}_\lambda\right)^{-1} \cdot \mathbf{T}_\lambda^T$$

which allows for the system matrix estimate to be formed by

$$\hat{\mathbf{A}}_\lambda = \mathbf{Y}_\lambda \cdot \mathbf{T}_\lambda^{\#}.$$

It is important to choose the known input angles of the reference polarizer such that the pseudo inverse can be found. In this calibration, a step size of 10° over the intervals $[0^\circ \ldots 90^\circ]$ and $[95^\circ \ldots 175^\circ]$ was found to yield good results. The application of this system matrix to convert the acquired imagery into Stokes imagery will be discussed in the next section.

2.3 Data Processing

Since each frame obtained from the sensor is collected at a different time, the frames must be registered to obtain accurate Stokes imagery. Data is collected in sets from the filter wheel where each set consists of four polarizer rotations for each spectral band thus giving a set size of 24 frames in the current configuration. The process of creating Stokes imagery requires accurate registration, so the four linear polarizer frames captured for each spectral band are registered using a Fourier-based method.[9] Next, the spectral bands are registered to create a set of imagery comprised of four polarizer orientations for each spectral band. Stokes imagery for each band is then created by application of the system matrix to the input imagery by

$$\hat{\mathbf{S}}_\lambda = \hat{\mathbf{A}}_\lambda^{\#} \cdot \mathbf{X}_\lambda$$

where $\hat{\mathbf{S}}_\lambda$ is a $(3 \times n_{pix})$ matrix which contains the best estimate of the Stokes imagery, $\hat{\mathbf{A}}_\lambda^{\#}$ is the pseudo inverse of the system matrix found during system calibration, and $\mathbf{X}_\lambda$ is the $(4 \times n_{pix})$ matrix of imagery collected by the system.

This data can be used in several different ways, depending on the application. In this preliminary study the anomaly detection routine TAD is applied to the combined spectral-Stokes stack.[10] This technique can produce both an anomaly detection map by utilizing the RX algorithm and a colorized representation of the different anomalous regions by utilizing the principal components transform.[11] Results from both approaches will be shown in Section 3. The registration and data combination process is outlined in Figure 5 which shows the workflow from raw frames to spectral Stokes imagery.

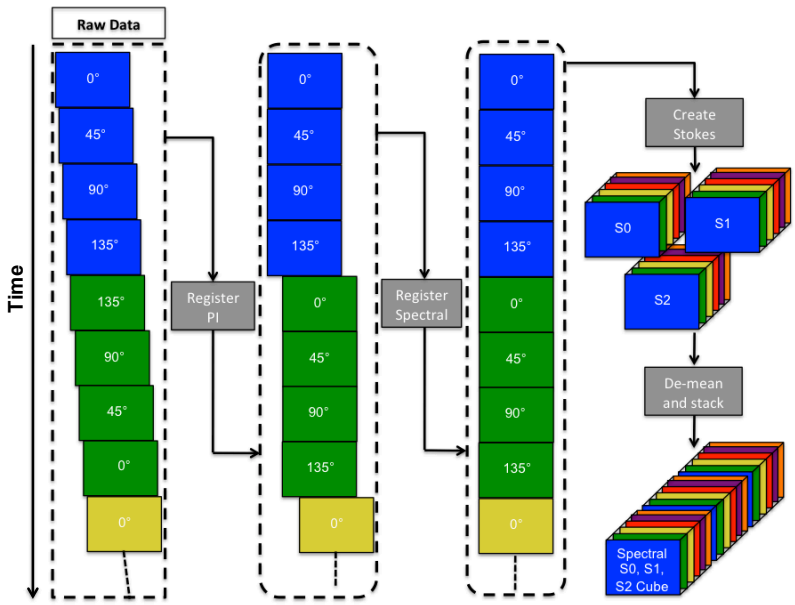

Figure 5: Flow chart for post-processing of MAPPS data. The polarimetric registration is performed first followed by registration of spectral bands. Spectral-Stokes cubes are then created.

3. PRELIMINARY RESULTS

Initial testing of the MAPPS system has been performed using two test scenes. The first scene was collected in the laboratory using a simplistic background, which provides a baseline for system performance. The second scene was collected from a building rooftop giving more complex illumination and scene clutter. In each case, the registration and data processing procedures were employed before the anomaly detection algorithm was applied.

3.1 Laboratory Scene

This scene was constructed using several different types of man-made objects placed on a dark felt cloth to provide a uniform background. A large aperture integrating sphere was used as a light source to provide adequate radiance onto the lab scene. Figure 6 shows an RGB image of the scene using the red, green, and blue S0 bands along with the S1 and S2 imagery from the green band. The S1 and S2 imagery was scaled such that higher grey levels correspond to positive Stokes values and darker grey levels correspond to negative Stokes values. The S1 image shows how the white painted objects tend to exhibit a large negative (vertically) polarized component due to radiance that undergoes internal volume scattering and is then transmitted back through the top layer, thus producing a vertically polarized orientation through Fresnel transmission. The black glossy surfaces have very little internal scattering and thus the predominant signal is first surface Fresnel reflection which is strongly positive (horizontally) polarized. The S2 image shows how the diagonal polarization signal changes sign across the camera field of view due in part to the large angular extent of the light source relative to the scene geometry. It should be noted that the objects were shifted during initial setup, which created a slightly different orientation of the felt. This changed the scattering properties of the disturbed regions compared to the rest of the felt which appears in the S2 image as a shadow or ghosting, but is actually due to the felt orientation. The TAD-RX anomaly detection map is also displayed which shows how all man-made objects appear anomalous compared to the black cloth background. In particular, the black car and Humvee models are easily detected which shows the potential benefit for collection of polarimetric information.

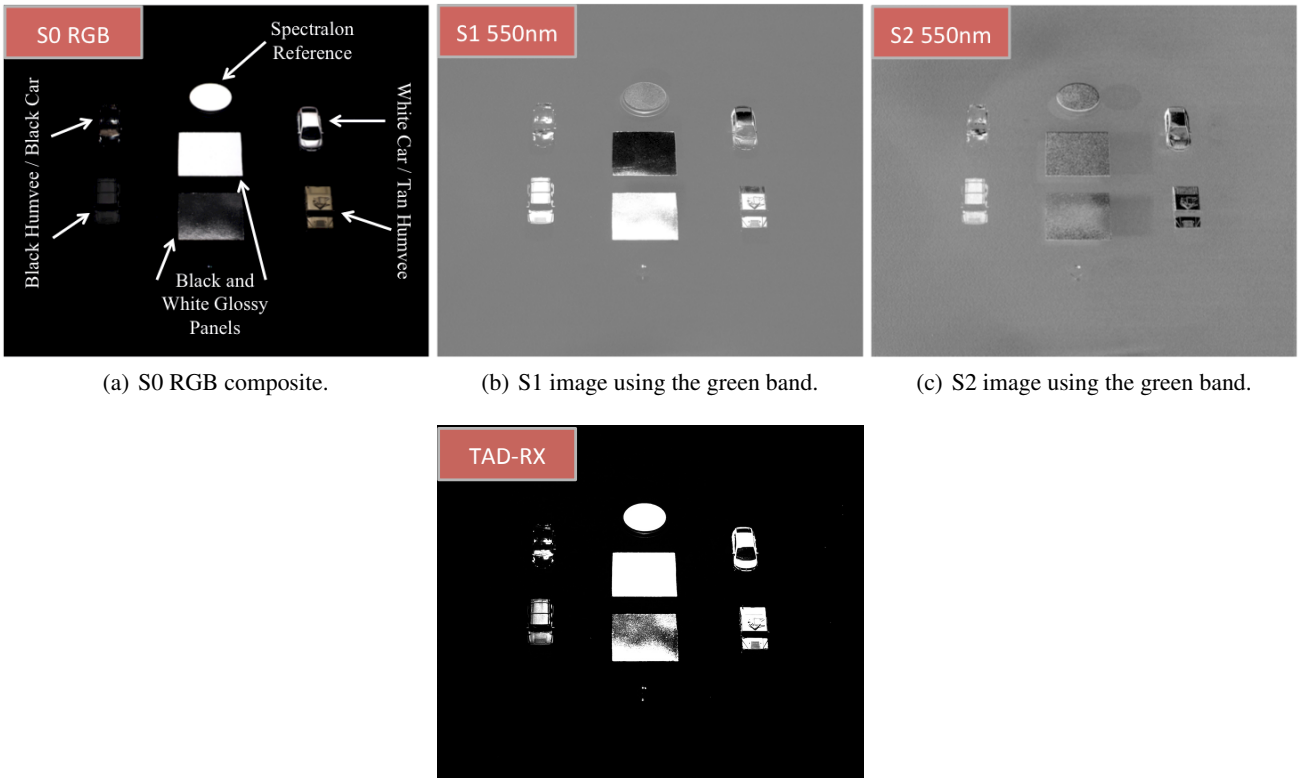

(a) S0 RGB composite. (b) S1 image using the green band. (c) S2 image using the green band.

(d) TAD-RX anomaly detection map.

Figure 6: Imagery of lab scene from MAPPS sensor of two painted panels, four model vehicles, and spectralon reference.

3.2 Rooftop Data

Imagery was also collected from the rooftop of a building to test the system in a more complex outdoor environment. A parking lot was imaged containing a mixture of asphalt and grass backgrounds along with a parked vehicle and a panel cluster.[12] The panel cluster has various painted regions comprising different surface finishes and colors. The panel surfaces can also be set a different angles to face different portions of the skydome. Figure 7 shows a cropped portion of the imagery that was captured in a backscattering geometry relative to the sun principle plane. The S1 and S2 imagery shows how the different panels have different Stokes values depending on which portion of the hemisphere is sampled with the given source / detector geometry. This is expected since the skydome has significant polarization.[13] The results of running TAD-PCA are also shown which indicate that various anomalous materials can be identified relative to the background parking lot and grass with this system.

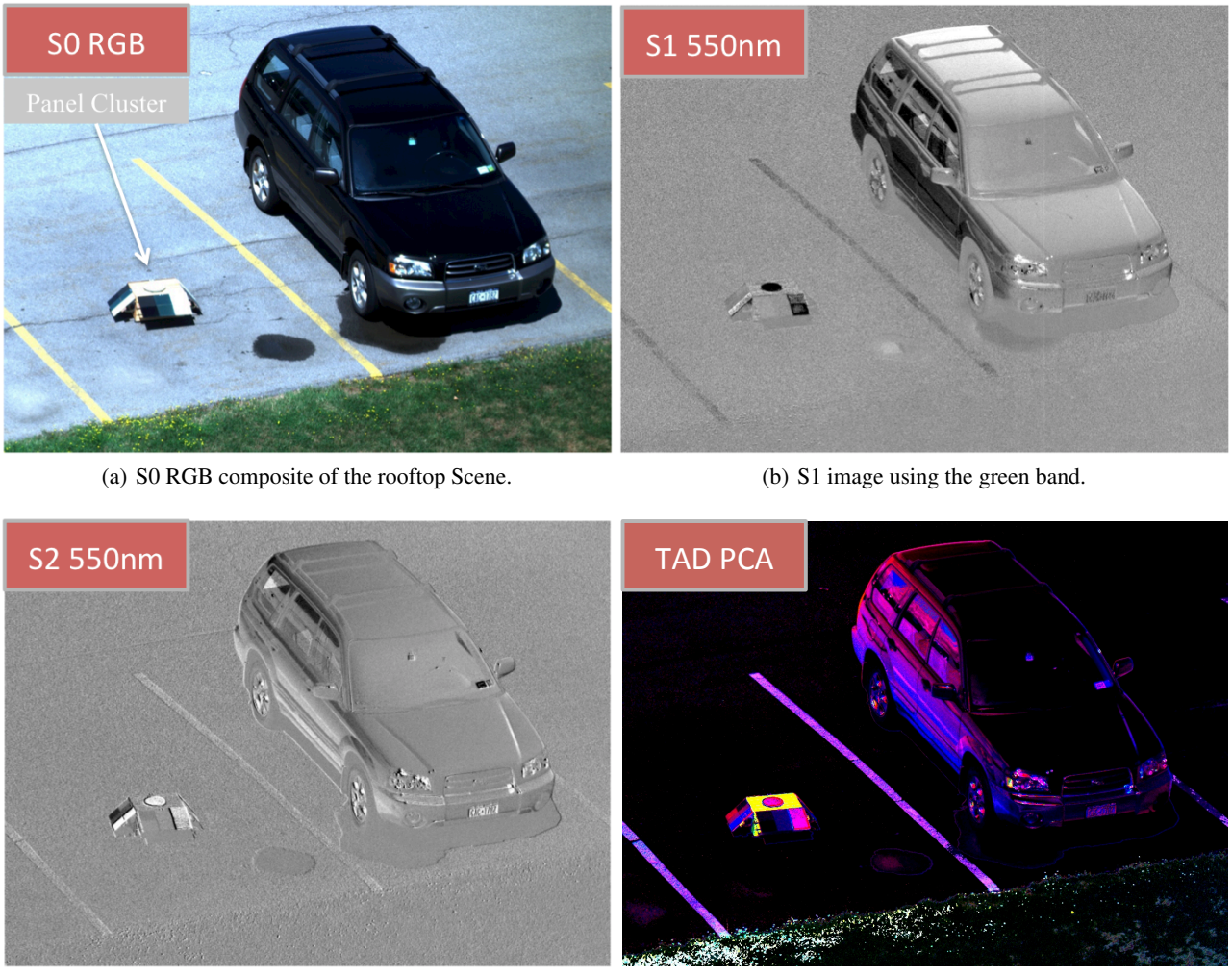

(a) S0 RGB composite of the rooftop Scene.

(b) S1 image using the green band.

(c) S2 image using the green band.

(d) TAD PCA anomaly detection results.

Figure 7: Rooftop scene imaged with MAPPS sensor.

4. CONCLUSIONS

A new imaging system, MAPPS, is presented which can collect spectro-polarimetric imagery through the use of a dual filter wheel. This system has been configured to collect four linear polarizer orientation for six different spectral bands that closely match the spectral response of the current generation WorldView 2 satellite. A workflow for data processing and

system calibration is presented which will allow for the creation of spectral-Stokes cubes from raw image data. Preliminary data from both the laboratory and an outdoor rooftop scene has shown that the system can produce imagery that contains polarimetric and spectral contrast. An anomaly detection algorithm has be run on the data showing the potential use for such a data set. Further work will revolve around collecting airborne imagery that will allow for the creation of test scenes to explore phenomenology and allow testing of new spectro-polarimetric algorithms.

5. ACKNOWLEDGEMENTS

The authors would like to thank Dr. Michael Gartley for his assistance in devising useful test scenes and describing the polarimetric effects observed as well as the Digital Imaging and Remote Sensing (DIRS) group at the Rochester Institute of Technology for generously providing funding for all hardware.

REFERENCES

[1] Schott, J. R., Brown, S. D., Raqueno, R. V., Gross, H. N., and Robinson, G., "Advanced synthetic image generation models and their application to multi/hyperspectral algorithm development," *Proc. SPIE* **3584**, 211–220 (1999). [doi:10.1117/12.339823].

[2] Rocchio, L. *The Landsat Program* (2011). http://landsat.gsfc.nasa.gov/.

[3] Lundeen, S. *AVIRIS - Airborne Visible / Infrared Imaging Spectrometer* (2011). http://aviris.jpl.nasa.gov/.

[4] d'Etudes Spatiales, C. N. *POLDER* (2007). http://smsc.cnes.fr/POLDER/.

[5] Snyder, D., Kerekes, J., Fairweather, I., Crabtree, R., Shive, J., and Hager, S., "Development of a web-based application to evaluate target finding algorithms," *IEEE Int. Geosci. Remote Sens. Symp.* **2**, II915–II918 (2009). [doi:10.1109/IGARSS.2008.4779144].

[6] Globe, D. *Worldview-2 Satellite* (2011). http://www.digitalglobe.com/index.php/88/WorldView-2.

[7] Walraven, R., "Polarization imagery," *Opt. Eng.* **20**(1), 14–18 (1981).

[8] Schott, J. R., [*Fundamentals of Polarimetric Remote Sensing*], vol. **TT81**, SPIE Tutorial Texts In Optical Engineering, SPIE Press, Bellingham, WA (2009). [doi:10.1117/3.817304].

[9] Persons, C. M., Chenault, D. B., Jones, M. W., Spradley, K. D., Gulley, M. G., Farlow, C. A., Goldstein, D. H., and Chenault, D. B., "Automated registration of polarimetric imagery using fourier transform techniques," *Polarization Measurement, Analysis, and Applications V* **4819**(1), 107–117, SPIE (2002). [doi:10.1117/12.450935].

[10] Bartlett, B. D. and Schlamm, A., "Anomaly detection with varied ground sample distance utilizing spectropolarimetric imagery collected using a liquid crystal tunable filter," *J. Appl. Remote Sens.* **50**(8), 081207 (2011). [doi:10.1117/1.3564818].

[11] Basener, W. F. and Messinger, D. W., "Enhanced detection and visualization of anomalies in spectral imagery," *Proc. SPIE* (7334), 73341Q (2009). [doi:10.1117/12.818672].

[12] Bartlett, B. D., Gartley, M. G., Messinger, D. W., Salvaggio, C., and Schott, J. R., "Spectro-polarimetric bidirectional reflectance distribution function determination of in-scene materials and its use in target detection applications," *J. Appl. Remote Sens.* **4**(043552), 1–21 (2010). [10.1117/1.3518394].

[13] Pust, N. J. and Shaw, J. A., "Comparison of skylight polarization measurements and modtran-p calculations," *J. Appl. Remote Sens.* **5**(1), 053529 (2011). [doi:10.1117/1.3595686].